

# Spiral patterns and biodiversity in lattice-free Lotka-Volterra models

P.P. Avelino,<sup>1,2</sup> D. Bazeia,<sup>3</sup> L. Losano,<sup>3</sup> J. Menezes,<sup>1,4</sup> and B.F. de Oliveira<sup>5</sup>

<sup>1</sup>*Instituto de Astrofísica e Ciências do Espaço, Universidade do Porto,  
CAUP, Rua das Estrelas, PT4150-762 Porto, Portugal*

<sup>2</sup>*Departamento de Física e Astronomia, Faculdade de Ciências,  
Universidade do Porto, Rua do Campo Alegre 687, PT4169-007 Porto, Portugal*

<sup>3</sup>*Departamento de Física, Universidade Federal da Paraíba 58051-900 João Pessoa, PB, Brazil*

<sup>4</sup>*Escola de Ciências e Tecnologia, Universidade Federal do Rio Grande do Norte  
Caixa Postal 1524, 59072-970, Natal, RN, Brazil*

<sup>5</sup>*Departamento de Física, Universidade Estadual de Maringá,  
Av. Colombo 5790, 87020-900 Maringá, PR, Brazil*

Stochastic simulations of cyclic three-species spatial predator-prey models are usually performed in square lattices with nearest neighbor interactions starting from random initial conditions. In this Letter we describe the results of novel lattice-free Lotka-Volterra stochastic simulations, showing that, contrary to previous claims, the emergence of spiral patterns does occur for sufficiently high values of the (conserved) total density of individuals. We also investigate the dynamics in our simulations, finding an empirical relation characterizing the dependence of the characteristic peak frequency and amplitude on the total density. Finally, we study the impact of the total density on the extinction probability, showing how a low population density may jeopardize biodiversity.

## I. INTRODUCTION

Cyclic predator-prey models, also known as rock-paper-scissors (RPS) models, have provided insight into some of the crucial mechanisms responsible for biodiversity [1–15] (see also [16–18] for the pioneer work by Lotka and Volterra, and May and Leonard). In their simplest version, spatial RPS models describe the space-time evolution of populations of three different species subject to nearest-neighbor cyclic predator-prey interactions. Simulations of spatial RPS models are usually performed on a square lattice (see, however, [19] for other lattice configurations). In three-state versions of these models each site is occupied by a single individual of one of the three species and there is a conservation law for the total number of individuals, or equivalently, for the total density (these models, involving simultaneous predation and reproduction, are known as Lotka-Volterra models [16, 17]). In four-state versions each site may either be occupied by a single individual or an empty space, and the total density is, in general, no longer conserved (see [20] for a case in which the number of individuals per site can be larger than unity and [21–30] for RPS generalizations involving an arbitrary number of species).

For small enough mobility rates, both three and four-state versions of spatial RPS models have been shown to lead to the stable coexistence of all three species. However, the complex spiralling patterns, observed in stochastic simulations of four-state spatial RPS models, appear to be absent in three-state versions. Furthermore, it has been claimed in [31] (see also [32–34]) that the emergence of stable spiral patterns cannot happen in the presence of a conservation law for the total density of individuals.

In this Letter we describe the results of novel lattice-free stochastic simulations of spatial RPS models, showing that spiral patterns may form in the case of a large

enough constant total density. We shall also investigate the dynamical properties of our simulations, quantifying the dependence of the characteristic peak frequency and amplitude on the total density, and study the impact that the total density may have on the conservation of biodiversity.

## II. LATTICE-FREE RPS SIMULATIONS

In our lattice-free stochastic simulations  $N_A$ ,  $N_B$  and  $N_C$  individuals of the species  $A$ ,  $B$  and  $C$ , respectively, are initially randomly distributed on a square-shaped box of linear size  $L = 1$  with periodic boundary conditions ( $N_A = N_B = N_C = N/3$  at the initial time). At each time step a randomly picked individual  $I$  of an arbitrary species  $S$  moves or preys with probability  $m$  or  $p = 1 - m$ , respectively. For the sake of definiteness, in this Letter we shall assume that both actions have the same probability of being selected ( $m = p = 1/2$ ). Nevertheless, we have verified that this particular choice does not have a significant impact on our main results.

Whenever mobility is selected, a random direction is chosen and the individual  $I$  moves in this direction by a distance  $\ell_m$ . On the other hand, if predation is selected then the individual  $I$  looks for the closest prey inside a circular area of radius  $\ell_p$  around itself and replaces it by an individual of its own species  $S$ . If no prey is found within this radius then the action is not executed. In this Letter we shall make the reasonable assumption that the mobility and predation length scales are identical ( $\ell = \ell_m = \ell_p$ ) and choose  $\ell = 2 \times 10^{-2}$  (we will later show that our main results are not affected by this specific choice). Note that, unlike in standard RPS lattice simulations, in our lattice-free simulations position swaps between neighbors never occur.

A generation timescale  $\Delta t = 1$  is defined as the time

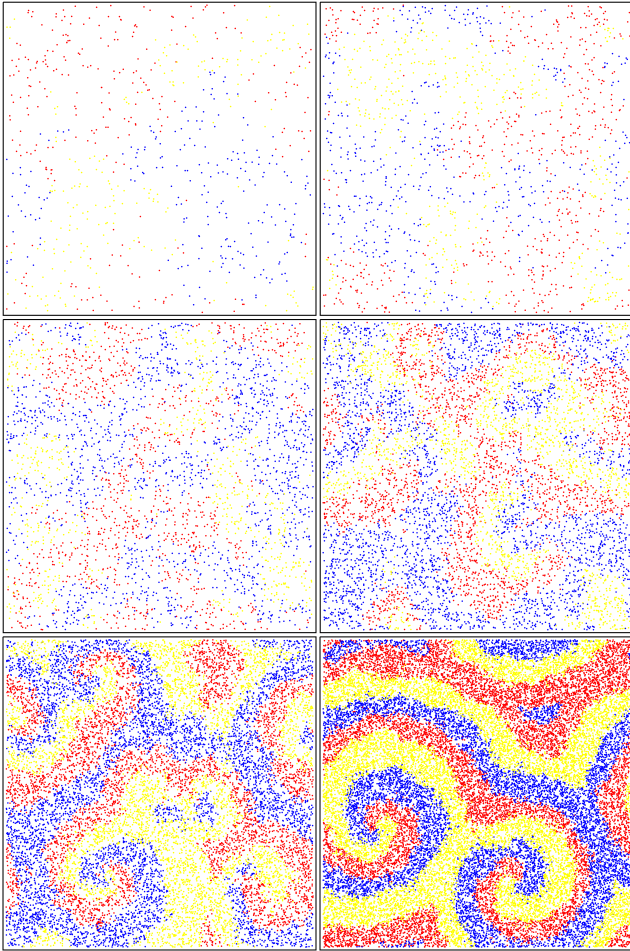


Figure 1: Snapshots of our lattice-free stochastic RPS simulations after  $t = 10^4$  generations, for six different values of the density parameter  $\varrho$  ( $\varrho = 7.0 \times 10^2$ ,  $1.5 \times 10^3$ ,  $3.2 \times 10^3$ ,  $6.7 \times 10^3$ ,  $1.4 \times 10^5$  and  $3.0 \times 10^5$ , from top to bottom and left to right, respectively)

necessary for  $N$  actions to be realized. In this Letter we consider simulations with different values of the (constant) density parameter  $\varrho = N/L^2$  in the interval  $[2.4 \times 10^1, 3 \times 10^5]$ . All simulations have a total duration of  $t = 1.5 \times 10^4$  generations.

### III. SPIRAL PATTERNS

Fig. 1 shows snapshots taken from six of our lattice-free RPS simulations with constant total densities  $\varrho = 7.0 \times 10^2$ ,  $1.5 \times 10^3$ ,  $3.2 \times 10^3$ ,  $6.7 \times 10^3$ ,  $1.4 \times 10^5$  and  $3.0 \times 10^5$  (from top to bottom and left to right, respectively) after  $t = 10^4$  generations.

Contrary to previous claims that spiral patterns would form only if the total density  $\varrho$  was not conserved [31], Fig. 1 shows that spiral patterns may indeed form for sufficiently large values of  $\varrho$ . On the other hand, Fig. 1 shows that spiral formation does not take place for small

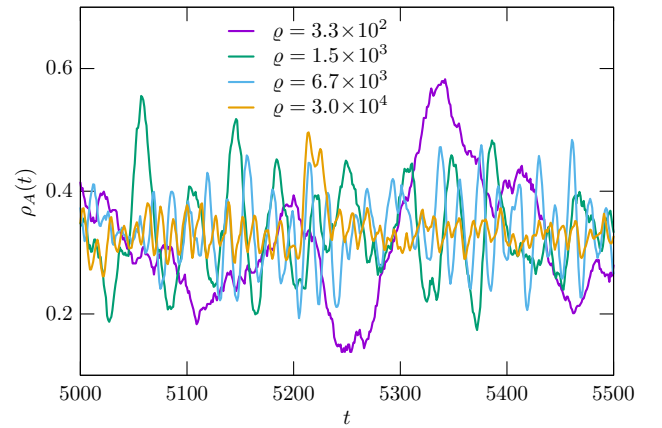


Figure 2: Time evolution of the fractional abundance of the species  $A$  for different values of the total density  $\varrho$  (a similar behavior is found for species  $B$  and  $C$ ).

values of  $\varrho$ .

If  $\ell \ll L$  and  $d = \varrho^{-1/2} \ll L$ , where  $d$  is the characteristic distance between neighbors, the size of the box does not have any significant impact on the patterns which emerge from the simulation, these being dependent essentially on the ratio  $q = \ell/d$ . Fig. 1 shows that spiral patterns are prominent only if  $q > 1$ . For  $q < 1$  the results appear to be consistent with those of the usual Lotka-Volterra stochastic simulations performed in square lattices with nearest neighbor interactions in which spiral formation is suppressed.

### IV. TIME EVOLUTION

The time evolution of the fractional abundance  $\rho_A = N_A/N$  of the species  $A$  is shown in Fig. 2 for different values of the density parameter  $\varrho$  (the results for species  $B$  and  $C$  are analogous — note that  $\rho_A + \rho_B + \rho_C = 1$ ). Fig. 2 shows that  $\rho_A$  oscillates with a characteristic time and amplitude which depends on the value of the total density  $\varrho$ . The larger the value of  $\varrho$ , the smaller the time (measured in units of one generation time) necessary for a predator to find its prey. Consequently, the frequency is a growing function of  $\varrho$ . On the other hand, since the oscillation amplitudes of the fractional abundances of the different species scale roughly with  $N^{-1/2}$  [35], the smaller the value of  $\varrho$ , the larger the characteristic oscillation amplitude of  $\rho_A$ .

The simultaneous representation of the time evolution of the fractional abundances of the three different species  $A$ ,  $B$  and  $C$  is shown in Fig. 3 for various values of the constant total density  $\varrho$ . The initial conditions are such that  $\rho_A = \rho_B = \rho_C = 1/3$ , thus implying that all orbits start at the center of the triangle. Fig. 3 shows that the smaller the value of  $\varrho$ , the larger the area of phase space occupied by the orbits. This implies that the probability of biodiversity being lost increases as  $\varrho$  is decreased, thus

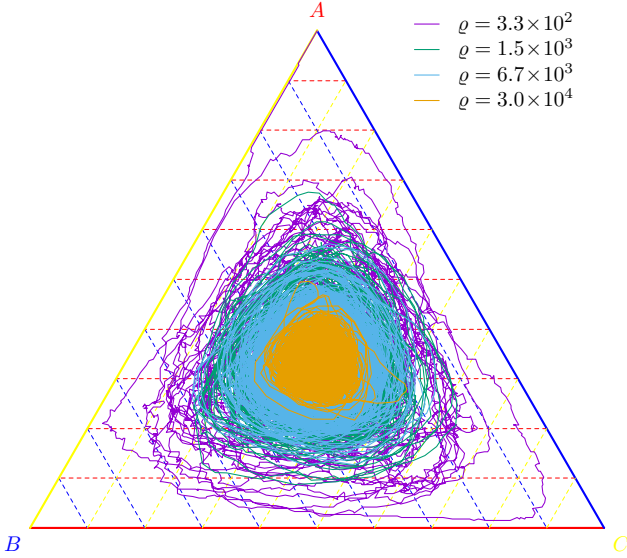


Figure 3: The ternary diagram shows the time evolution of the fractional abundances of the three different species on single runs of our simulations for different values of the total density  $\rho$ . For  $\rho = 3.3 \times 10^2$  only the species  $A$  remains by the end of the simulation.

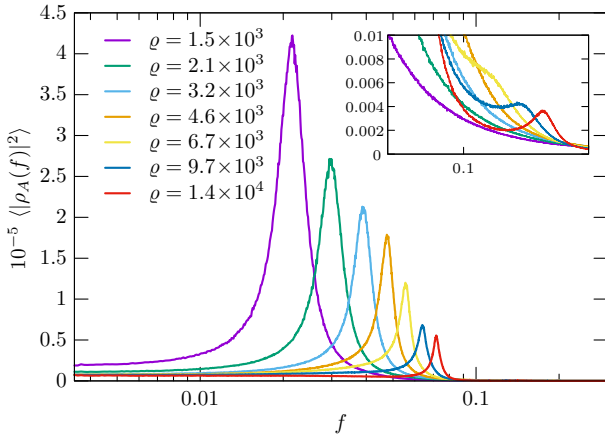


Figure 4: Power spectrum of  $\rho_A$  for different values of the total density  $\rho$ . The results were averaged over  $5 \times 10^3$  simulations with a time span  $t = 1.5 \times 10^4$  generations of different initial conditions (the first  $5 \times 10^3$  generations of each simulation have been discarded in the calculation of the power spectrum).

showing that the impact of the increase of the characteristic oscillation amplitude (as  $\rho$  is decreased) is significantly larger than that of the increase of the characteristic period (or of the consequent reduction of the number of cycles within the simulation time span). In particular, for  $\rho = 3.3 \times 10^2$  only the species  $A$  remains by the end of the simulation, even though it was on the verge of extinction for several periods before that.

In order to provide a more quantitative description of the time evolution of the system we compute the Fourier transform of the fractional abundance  $\rho_A(t)$  of the species

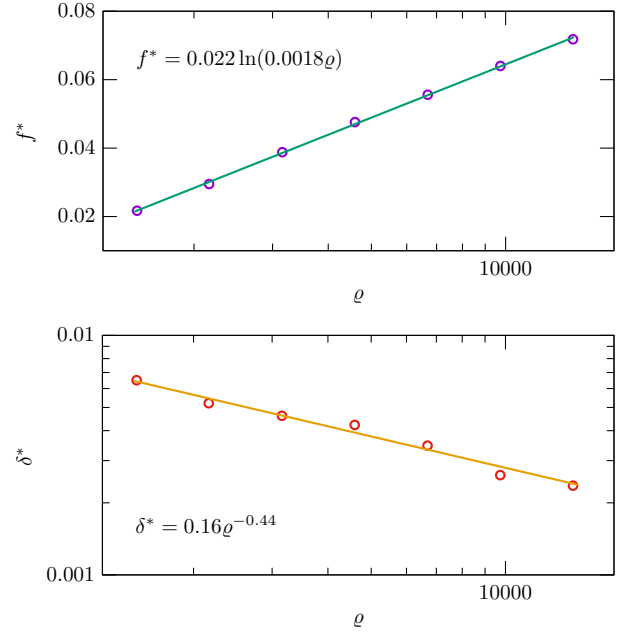


Figure 5: Dependence of the peak frequency  $f^*$  (upper panel) and amplitude  $\delta^*$  (lower panel) on the total density  $\rho$ . The solid lines represent the fitting functions.

A. Let us define the temporal discrete Fourier transform as

$$\rho_A(f) = \frac{1}{N} \sum_{t=0}^{N_G} \rho_A(t) e^{-2\pi i f t}, \quad (1)$$

where  $f = t/N_G$  with  $t = [5 \times 10^3, N_G]$  and  $N_G = 1.5 \times 10^4$  generations.

The power spectrum of  $\rho_A$  is displayed in Fig. 4 for different values of the total density  $\rho$ . The results shown in Fig. 4 were averaged over  $5 \times 10^3$  simulations with a time span  $t = 1.5 \times 10^4$  generations and different initial conditions (the first  $5 \times 10^3$  generations of each simulation have been discarded in the calculation of the power spectrum). The insert of Fig. 4 also reveals a second peak for high enough values of the total density  $\rho$ . This is related with the very fast oscillations with small amplitudes also found in [26].

As expected from the previous discussion, the characteristic peak frequency  $f^*$ , defined as the value of the frequency  $f$  at the maximum of the power spectrum, increases, while the characteristic peak amplitude, defined by  $\delta^* = (\langle |\rho_A(f^*)|^2 \rangle)^{1/2}$ , decreases with  $\rho$ . Fig. 5 shows the dependence of  $f^*$  (upper panel) and  $\delta^*$  (lower panel) on the total density  $\rho$ , where an empirical fit to the results showing a logarithmic dependence (in the case of  $f^*$ ) and a power law dependence (in the case of  $\delta^*$ ) is also given.

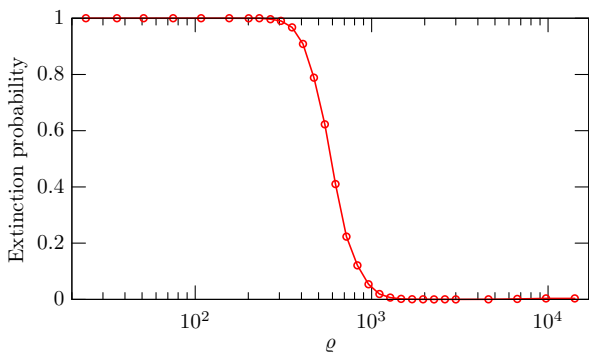


Figure 6: The extinction probability as a function of the total density  $\rho$ . The results were obtained from  $5 \times 10^3$  simulation runs for each data point.

## V. AVERAGE DENSITY AND BIODIVERSITY

The impact of mobility on biodiversity has been investigated in detail using simulations performed in square lattices with nearest neighbor interactions. In these simulations the ratio  $q = \ell/d$  is always equal to unity. We now consider the impact of the total density  $\rho$  on the extinction probability (for a fixed  $\ell = 0.02$ ) using our lattice-free simulations, which allow for a variable ratio  $q = \ell/d$ . To this end we have performed a set of  $5 \times 10^3$  simulations for different values of the total density  $\rho$  and verified whether or not one or more species was extinct after  $1.5 \times 10^4$  generations. Fig. 6 depicts the extinction probability as function of total density  $\rho$ . It shows that biodiversity is maintained only above a critical value of the total density  $\rho_c = (2.3 \pm 0.2) \times 10^2$ , with the transition between the coexistence and extinction regimes be-

ing quite sharp.

## VI. CONCLUSIONS

In this Letter we reported on the results of novel lattice-free stochastic simulations of cyclic three-species spatial predator-prey models with a conserved total density. We have shown that, contrary to previous claims, spiral patterns do form in these simulations for high values of the total density (that is, for values of the ratio  $q = \ell/d$  greater than unity). We have taken advantage of the freedom to vary  $q$  in our simulations to study the impact of the total density on population dynamics (for a fixed  $\ell$ ), showing that the characteristic peak frequency and amplitude display, respectively, a logarithmic increase and a power law decrease with the total density. Finally, we have shown that coexistence can only be maintained above a critical value of the total density, with only a narrow transition region between biodiversity and extinction regimes, which indicates that even moderate changes on the total density of individuals may have a great impact on the conservation of biodiversity.

## ACKNOWLEDGMENTS

We thank CAPES, CNPq, FAPERJ, FCT, Fundação Araucária, and INCT-FCx for financial and computational support. PPA acknowledges support from FCT Grant UID/FIS/04434/2013, DB acknowledges support from Grants CNPq:455931/2014-3 and CNPq:306614/2014-6, and LL acknowledges support from Grants CNPq:307111/2013-0 and CNPq:447643/2014-2.

- 
- [1] B. Kerr, M. A. Riley, M. W. Feldman, and B. J. M. Bohannan, *Nature* **418**, 171 (2002).
  - [2] B. C. Kirkup and M. A. Riley, *Nature (London)* **428**, 412 (2004).
  - [3] T. Reichenbach, M. Mobilia, and E. Frey, *Phys. Rev. E* **74**, 051907 (2006).
  - [4] G. Szabó and G. Fáth, *Phys. Rep.* **446**, 97 (2007).
  - [5] T. Reichenbach, M. Mobilia, and E. Frey, *Nature* **448**, 1046 (2007).
  - [6] T. Reichenbach, M. Mobilia, and E. Frey, *Phys. Rev. Lett.* **99**, 238105 (2007).
  - [7] T. Reichenbach, M. Mobilia, and E. Frey, *Journal of Theoretical Biology* **254**, 368 (2008).
  - [8] E. Frey, *Physica A: Statistical Mechanics and its Applications* **389**, 4265 (2010).
  - [9] Q. He, M. Mobilia, and U. C. Täuber, *Phys. Rev. E* **82**, 051909 (2010).
  - [10] Q. He, M. Mobilia, and U. C. Täuber, *The European Physical Journal B* **82**, 97 (2011).
  - [11] L.-L. Jiang, T. Zhou, M. Perc, and B.-H. Wang, *Phys. Rev. E* **84**, 021912 (2011).
  - [12] A. Dobrinevski and E. Frey, *Phys. Rev. E* **85**, 051903 (2012).
  - [13] J. Knebel, T. Krüger, M. F. Weber, and E. Frey, *Phys. Rev. Lett.* **110**, 168106 (2013).
  - [14] J. Vukov, A. Szolnoki, and G. Szabó, *Phys. Rev. E* **88**, 022123 (2013).
  - [15] A. Szolnoki and M. Perc, *Scientific Reports* **6**, 38608 (2016).
  - [16] A. J. Lotka, *Proceedings of the National Academy of Science* **6**, 410 (1920).
  - [17] V. Volterra, *Nature (London)* **118**, 558 (1926).
  - [18] R. May and W. Leonard, *SIAM Journal on Applied Mathematics* **29**, 243 (1975).
  - [19] A. Szolnoki and G. Szabó, *Phys. Rev. E* **70**, 037102 (2004).
  - [20] M. J. Washenberger, M. Mobilia, and U. C. Täuber, *Journal of Physics: Condensed Matter* **19**, 065139 (2007).
  - [21] G. Szabó, A. Szolnoki, and I. Borsos, *Phys. Rev. E* **77**, 041919 (2008).
  - [22] S. Allesina and J. M. Levine, *PNAS* **108**, 5638 (2011).

- [23] C. H. Durney, S. O. Case, M. Pleimling, and R. K. P. Zia, *Phys. Rev. E* **83**, 051108 (2011).
- [24] P. P. Avelino, D. Bazeia, L. Losano, and J. Menezes, *Phys. Rev. E* **86**, 031119 (2012).
- [25] P. P. Avelino, D. Bazeia, L. Losano, J. Menezes, and B. F. Oliveira, *Phys. Rev. E* **86**, 036112 (2012).
- [26] A. Roman, D. Dasgupta, and M. Pleimling, *Phys. Rev. E* **87**, 032148 (2013).
- [27] P. P. Avelino, D. Bazeia, J. Menezes, and B. F. de Oliveira, *Physics Letters A* **378**, 393 (2014).
- [28] P. P. Avelino, D. Bazeia, L. Losano, J. Menezes, and B. F. de Oliveira, *Phys. Rev. E* **89**, 042710 (2014).
- [29] A. Szolnoki, M. Mobilia, L.-L. Jiang, B. Szczeny, A. M. Rucklidge, and M. Perc, *Journal of The Royal Society Interface* **11**, 20140735 (2014).
- [30] P. P. Avelino, D. Bazeia, L. Losano, J. Menezes, and B. F. de Oliveira, *Physics Letters A* **381**, 1014 (2017).
- [31] M. Peltomäki and M. Alava, *Phys. Rev. E* **78**, 031906 (2008).
- [32] T. Reichenbach and E. Frey, *Phys. Rev. Lett.* **101**, 058102 (2008).
- [33] B. Szczeny, M. Mobilia, and A. M. Rucklidge, *EPL (Europhysics Letters)* **102**, 28012 (2013).
- [34] B. L. Brown and M. Pleimling, *Phys. Rev. E* **96**, 012147 (2017).
- [35] T. Tomé, Á. L. Rodrigues, E. Arashiro, and M. J. de Oliveira, *Computer Physics Communications* **180**, 536 (2009).